

Delayed Expulsion of the Nematode *Trichinella spiralis* in Mice Lacking the Mucosal Mast Cell-specific Granule Chymase, Mouse Mast Cell Protease-1

By Pamela A. Knight,* Steven H. Wright,* Catherine E. Lawrence,‡
Yvonne Y.W. Paterson,‡ and Hugh R.P. Miller*

From the *Department of Veterinary Clinical Studies, Royal (Dick) School of Veterinary Studies, and Wellcome Trust Centre for Research in Comparative Respiratory Medicine, University of Edinburgh, Easter Bush Veterinary Centre, Midlothian EH25 9RG, United Kingdom; and the ‡Department of Immunology, Strathclyde Institute of Biological Sciences, Glasgow G4 0NR, United Kingdom

Abstract

Expulsion of gastrointestinal nematodes is associated with pronounced mucosal mast cell (MMC) hyperplasia, differentiation, and activation, accompanied by the systemic release of MMC granule chymases (chymotrypsin-like serine proteases). The β -chymase mouse mast cell protease-1 (mMCP-1) is expressed predominantly by intraepithelial MMCs, and levels in the bloodstream and intestinal lumen are maximal at the time of worm expulsion in parasitized mice. To address the *in vivo* functions of MMC-specific β -chymases, we have generated transgenic mice that lack the mMCP-1 gene. They were backcrossed onto a congenic BALB/c background to investigate the response to nematode infection. The deletion of the mMCP-1 gene is associated with significantly delayed expulsion of *Trichinella spiralis* and increased deposition of muscle larvae in BALB/c mice despite the presence of normal and sometimes increased numbers of MMCs. Neither worm fecundity nor worm burdens were altered in *Nippostrongylus*-infected mMCP-1^{-/-} BALB/c mice. These data demonstrate, for the first time, that the ablation of an MMC-derived effector molecule compromises the expulsion process.

Key words: mucosal immunity • mast cell hyperplasia • helminth parasite • submucosa • *Nippostrongylus brasiliensis*

Introduction

Mast cells are frequently found at interfaces with the external environment, where they participate in a wide array of immunoregulatory functions, including tissue inflammatory reactions to pathogens. Mucosal mast cells (MMC) in the pulmonary and gastrointestinal tracts are distinct from mast cells in other tissues in their biochemical and functional properties and in their content of neutral granule serine proteases (1–4). Pronounced hyperplasia, differentiation, and activation of MMCs occurs in the gut during nematode infections (5, 6). In rodents and sheep, this is associated with the systemic release of MMC granule chymases (chymotrypsin-like serine proteases) at the time of worm expulsion (6). The MMC-specific β -chymase rat mast cell protease-II (rMCP-II) promotes intestinal epithelial perme-

ability by an as yet undefined mechanism that may involve proteolysis of tight junction proteins (7, 8). It was suggested that a general function for β -chymases may be to increase gut permeability and permit the transfer of antibodies and other plasma proteins into the niche occupied by the parasite (7, 8). A homologous β -chymase, mouse mast cell protease-1 (mMCP-1), is expressed by MMCs that are predominantly located within the epithelium (9). mMCP-1 is expressed constitutively, but levels increase in the bloodstream and intestinal lumen of parasitized mice and are maximal at the time of worm expulsion (10). It is possible, therefore, that rMCP-II, mMCP-1, and sheep mast cell protease-1, all of which are released systemically and into the gut lumen (6, 7, 10), participate in the effector response to intestinal nematodes.

To address the *in vivo* functions of MMC-specific β -chymases, we have generated transgenic mice that lack the mMCP-1 gene (11). Preliminary experiments where mMCP-1^{-/-} mice were infected with the intestinal nema-

Address correspondence to P.A. Knight, Dept. of Veterinary Clinical Studies, Royal (Dick) School of Veterinary Studies, Easter Bush Veterinary Centre, Roslin, Midlothian EH25 9RG, UK. Phone: 44-31-650-7698; Fax: 44-31-650-7697; E-mail: pam.knight@vet.ed.ac.uk

to *Nippostrongylus brasiliensis* resulted in altered MMC hyperplasia compared with infected mMCP-1^{+/+} controls, although it was not clear whether these differences were due to deletion of mMCP-1 or to the different immunological backgrounds of the two groups of mice (11). We have now backcrossed the mMCP-1^{-/-} and mMCP-1^{+/+} mice for 7–10 generations onto a BALB/c background, a strain in which the kinetics of expulsion of *N. brasiliensis* and other intestinal nematodes have been extensively described. While rejection of *N. brasiliensis* appears to be through mast cell independent mechanisms (12), there is clear evidence that mast cells are central to the expulsion of *Trichinella spiralis* (13, 14). Here we investigate the kinetics of expulsion of both *N. brasiliensis* and *T. spiralis* and the accompanying MMC hyperplasia in congenic BALB/c mMCP-1^{-/-} and mMCP-1^{+/+} mice.

Materials and Methods

Transgenic Mice. The generation of mMCP-1^{-/-} transgenic mice has been described (11). mMCP-1^{+/+} mice were backcrossed from their original MF-1/129/C57BL/6 mixed background onto a BALB/c background for 10 generations and used to generate congenic mMCP-1^{-/-} and mMCP-1^{+/+} BALB/c F₁₀ lines. All experiments were done in accordance with the Animals (Scientific Procedures) Act, 1986.

Parasite Infections. To assess responses to intestinal nematode infection, groups of age- and sex-matched (50:50 males/females per group) mMCP-1^{-/-} and mMCP-1^{+/+} 8–12-wk-old BALB/c F₇ or BALB/c F₁₀ mice were infected with either *N. brasiliensis* or *T. spiralis* (see below) and killed by halothane inhalation at specific intervals after infection. Samples of jejunum were removed starting 10 cm from the pylorus for ELISAs (1 cm), histology (3 cm), and RNA purification (0.5 cm), respectively, and the remainder of the small intestine was used for adult worm isolation. Maintenance and recovery of the mouse-adapted strain of *N. brasiliensis* (donated by Dr. J. Urban, U.S. Department of Agriculture, Beltsville, MD) has been described previously (11). For primary infections, mice were inoculated subcutaneously with 500 L3 larvae per mouse. Adult worms for secondary challenge were isolated from BALB/c mice 7 d after infection by Baerman's technique and separated from gut contents by centrifugation at 1,250 g through 100% Histopac (Sigma-Aldrich) for 5 min. Adult worms were aspirated from the upper layer and resuspended in PBS/0.1% agar. Mice were each inoculated with 200 adult worms by gavage 21 d after infection. Both primary and challenge infections were monitored daily by fecal egg counts.

Maintenance, infection, and recovery of *T. spiralis* larvae was based on standard methods (15). Mice were infected by gavage with 300–500 muscle larvae in 0.2 ml of PBS/0.1% agar freshly isolated from muscle cysts from 30–90 d infected BALB/c mice. Challenge infections were with 200–300 larvae 3 wk after infection. Numbers of encysted muscle larvae 30+ d after infection were calculated from tissue digests from individual cadavers (five to six per group) (15). Adult worms were isolated by opening freshly isolated small intestine longitudinally, transferring to a 1-mm-mesh sieve in 100 ml of HBSS (GIBCO BRL), and incubating for 4 h at 37°C. Migrated worms were aspirated and fixed in 1% paraformaldehyde. Parasites were enumerated from five to six mice per group per time point, and data were compared using the nonparametric Mann-Whitney two-tailed test using statistical/

graphical software (Microsoft Prism) with a significance level of $P < 0.05$.

Histochemistry and Immunohistochemistry. For histology, 2–3-cm lengths of jejunum were rolled, villi outermost using the Swiss roll technique, and fixed in Carnoy's before subsequent processing and sectioning (11). Mast cells were detected by staining sections from Carnoy's-fixed tissue overnight in 0.5% Toluidine Blue (Merck) in 0.5 mol/liter HCl, pH 0.5, and counterstaining for 1 s in 1% eosin solution (Surgipath) as described previously (11). The distribution of mast cells in the epithelium, lamina propria, submucosa, and muscularis was compared in equivalent areas of jejunum from five to six mice per time point. Toluidine Blue-positive mast cells in the epithelium and lamina propria were enumerated in 20 villus-crypt units (vcu) (16) and in the submucosa/muscularis regions directly below 20 vcu. Numbers of mast cells in all regions were calculated and expressed per vcu, and data were compared using the nonparametric Mann-Whitney test as above.

Quantification of mMCP-1. Concentrations of mMCP-1 in snap-frozen jejunum (micrograms per gram wet weight) and in serum (nanograms per milliliter) were assayed using the rat monoclonal RF6.1-based ELISA (9) with modifications; affinity-purified monoclonal RF6.1 (5 µg/ml) was the capture antibody, and polyclonal sheep anti-mMCP (2 µg/ml) (11) was used for detection of bound mMCP-1. Bound antibody was visualized using donkey anti-sheep IgG horseradish peroxidase conjugate (Sigma-Aldrich) at 1:8,000.

Detection of mMCP-1, mMCP-2, and mMCP-5 Transcripts by Reverse Transcription PCR. 0.5-cm samples of jejunum were transferred into 0.5 ml of RNA-later™ reagent (Ambion, Inc.) and were stored at 4°C overnight and then at -20°C until processing. Samples were homogenized on ice in 2 ml of Tri-Reagent™ (Sigma-Aldrich) using a tissue homogenizer, and total RNA was isolated as described previously (17). Contaminating DNA was removed by incubating 5 µg of total RNA with 6 U of DNA-free™ DNase (Ambion, Inc.) in 50-µl volumes of 10 mM Tris-HCl, pH 7.5, 2.5 mM MgCl₂, and 0.1 mM CaCl₂ for 1 h at 37°C before inactivation using 0.1 volume DNA-free™ DNase Inactivation Reagent. 1 µg of RNA was reverse transcribed and amplified by PCR using gene-specific primers for mMCP-1, mMCP-2, and mMCP-5 as previously described (11). Primers for mouse glyceraldehyde-3-phosphate dehydrogenase (GAPDH), 5'-GAAGGGCTCATGACCACAGTCCATG (5' primer) and 3'-TGTTGCTGTAGCCGTATTCATTGTC (3' primer), were purchased from Stratagene. 1/20th volume cDNA from the reverse transcription reaction was amplified for 1 min at 94°C, 2 min at 63°C, and 3 min at 72°C for 16, 20, 24, and 28 thermocycles before stopping the reaction at -20°C, with equivalent quantities of non-reverse-transcribed RNA as negative controls. PCR products were visualized on ethidium bromide-stained 1.2% agarose gels, and images were recorded using a Kodak Digital Science™ Image Station 440CF and 1D Image Analysis software.

Results

mMCP-1^{-/-} Mice Show a Reduced Ability to Expel Primary *T. spiralis* Infections. The responses of mMCP-1^{-/-} mice to primary infections with *T. spiralis* were examined. Mice in both mMCP-1^{-/-} and mMCP-1^{+/+} groups were infected with 500 *T. spiralis* larvae, and worm burdens were assessed 6, 14, and 18 d later ($n = 6$). By day 18, mice in

both groups had reduced worm burdens, but the numbers of worms were significantly greater ($P < 0.01$, Mann-Whitney test) in the mMCP-1^{-/-} mice compared with the mMCP-1^{+/+} controls (Fig. 1 A).

The delayed expulsion of *T. spiralis* in the absence of mMCP-1 was further confirmed in fully congenic BALB/c F₁₀ mMCP-1^{-/-} and mMCP-1^{+/+} mice. In this experiment, the infective dose was reduced from 500 to 300 muscle larvae, and 5 rather than 2 time points were chosen over the expected expulsion period (days 12–16) (18). Mice in both groups were infected with 300 *T. spiralis* muscle larvae, and worm burdens were assessed 1, 6, 13, 14, 15, and 16 d later ($n = 5–6$; Fig. 1 B). The recovery of worms on days 1 and 6 showed that the larvae established normally in both groups and that the population remained stable until days 13 and 14 (Fig. 1 B). However, on days 15 and 16, expulsion was complete in five out of six of the mMCP-1^{+/+} mice, whereas four of six mMCP-1^{-/-} mice still carried worm burdens (day 15, $P < 0.01$; Day 16, $P < 0.05$; Fig. 1 B). Similarly, when muscle larval burdens were assessed 30 d after infection, there were significantly larger

($P < 0.01$) numbers in the mMCP-1^{-/-} than in the mMCP-1^{+/+} mice (Fig. 1 B), a finding that was confirmed in two other experiments (data not shown).

mMCP-1^{-/-} Mice Expel Secondary *T. spiralis* Infections Less Efficiently. To assess the response to a challenge infection with *T. spiralis*, BALB/c F₁₀ mMCP-1^{-/-} and mMCP-1^{+/+} mice were each infected with 300 muscle larvae and were reinfected with an additional 300 larvae 21 d later. As controls for the challenge infections, age- and sex-matched naive mMCP-1^{-/-} and mMCP-1^{+/+} mice were simultaneously infected with 300 larvae from the same preparation. Worm burdens were assessed 6 d after each infection (Fig. 2 A). mMCP-1^{-/-} and mMCP-1^{+/+} mice immunized by infection 21 d before secondary challenge had reduced worm burdens compared with the unimmunized controls (Fig. 2 A). There was, however, a significantly larger ($P < 0.05$) worm burden in the immunized mMCP-1^{-/-} mice when compared with the mMCP-1^{+/+} controls (Fig. 2 A).

The Expulsion of *N. brasiliensis* Occurs Normally in mMCP-1^{-/-} Mice. Preliminary experiments investigating *N. brasiliensis* infections in MF-1/129/C57BL/6 mMCP-1^{-/-}

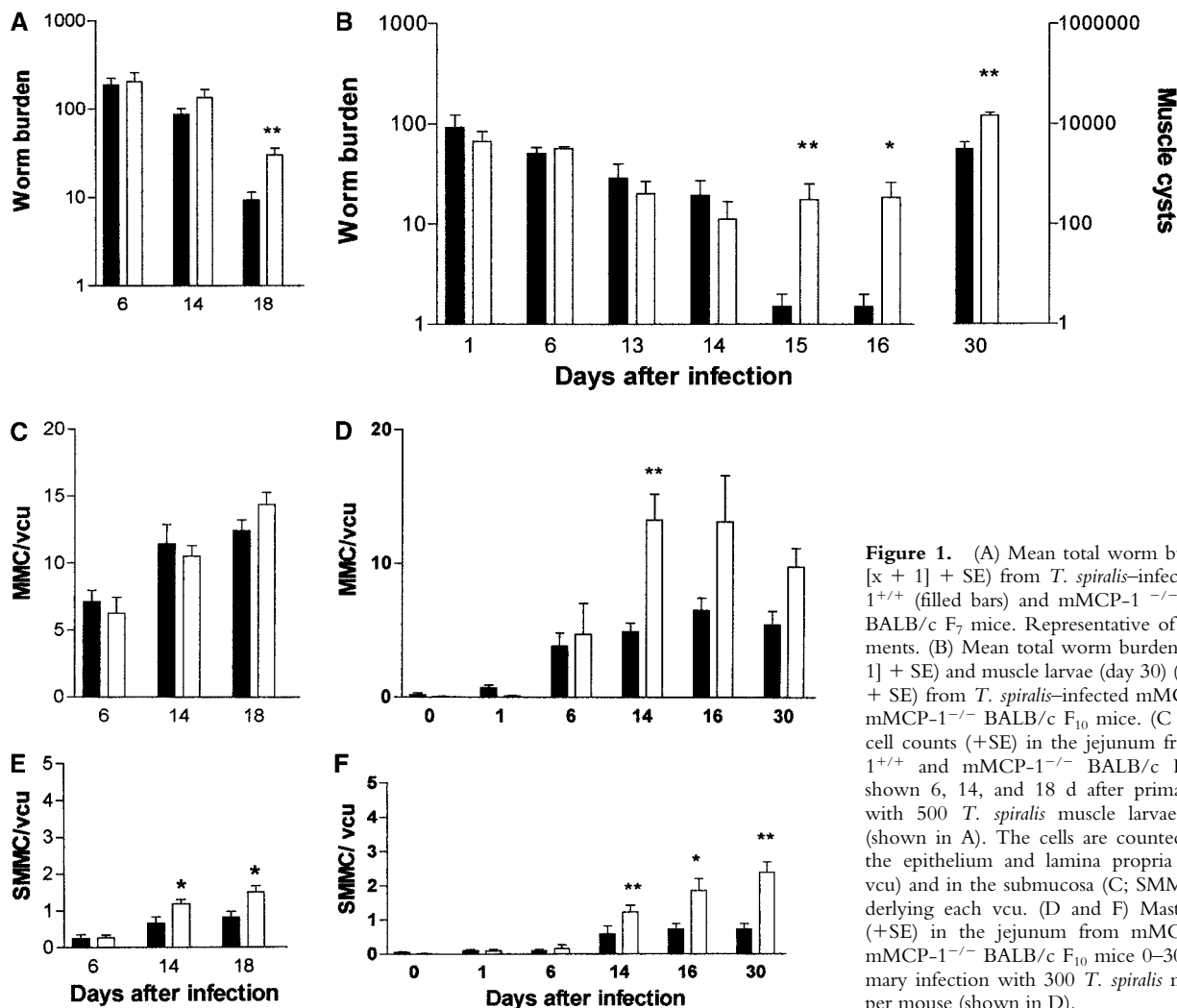


Figure 1. (A) Mean total worm burdens ($\log_{10} [x + 1] + SE$) from *T. spiralis*-infected mMCP-1^{+/+} (filled bars) and mMCP-1^{-/-} (open bars) BALB/c F₇ mice. Representative of two experiments. (B) Mean total worm burdens ($\log_{10} [x + 1] + SE$) and muscle larvae (day 30) ($\log_{10} [x + 1] + SE$) from *T. spiralis*-infected mMCP-1^{+/+} and mMCP-1^{-/-} BALB/c F₁₀ mice. (C and E) Mast cell counts (+SE) in the jejunum from mMCP-1^{+/+} and mMCP-1^{-/-} BALB/c F₇ mice are shown 6, 14, and 18 d after primary infection with 500 *T. spiralis* muscle larvae per mouse (shown in A). The cells are counted per vcu in the epithelium and lamina propria (B; MMC/vcu) and in the submucosa (C; SMMC/vcu) underlying each vcu. (D and F) Mast cell counts (+SE) in the jejunum from mMCP-1^{+/+} and mMCP-1^{-/-} BALB/c F₁₀ mice 0–30 d after primary infection with 300 *T. spiralis* muscle larvae per mouse (shown in D).

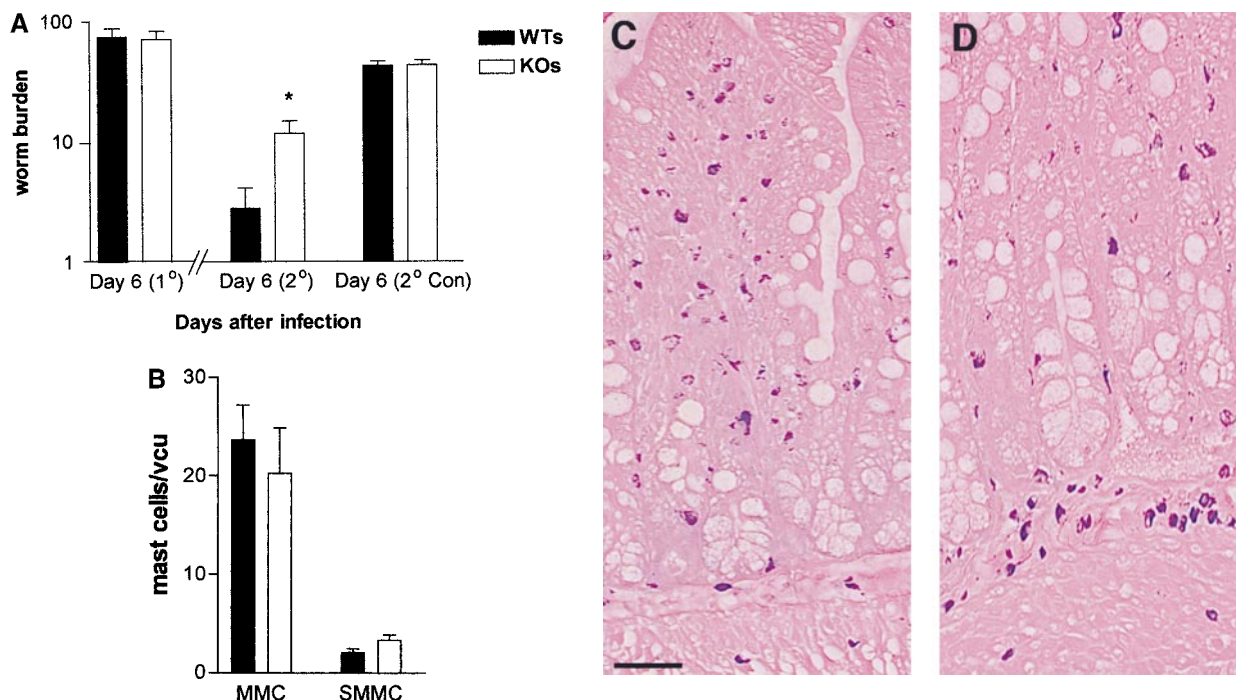


Figure 2. (A) Mean worm burdens ($\log_{10}[x + 1] + SE$) in mMCP-1^{+/+} and mMCP-1^{-/-} BALB/c F₁₀ mice after primary infection on day 0 (1°) and challenge infection on day 21 (2°) with 300 *T. spiralis* muscle larvae per mouse. Data are shown 6 d after an initial primary infection (day 6 [1°]), 6 d after receiving the challenge dose (day 6 [2°]), and from an equivalent naive group that received the challenge dose only (day 6 [2° Con]). (B) Mast cell counts (+SE) in the jejunum from mMCP-1^{+/+} (WTs) and mMCP-1^{-/-} (KOs) BALB/c F₁₀ mice are shown 6 d after challenge infection with *T. spiralis* (shown in A). See legend for Fig. 1, C and E. (C and D) Toluidine blue/eosin-stained jejunum from mMCP-1^{+/+} (C) and mMCP-1^{-/-} (D) BALB/c F₁₀ mice 6 d after challenge with *T. spiralis*. The reduced intensity of staining of MMCs in the villi in mMCP-1^{-/-} jejunum is in accordance with previous data (11). Note the abundant mast cells in the submucosa of the mMCP-1^{-/-} jejunum compared with that of mMCP-1^{+/+} jejunum.

mice demonstrated that although worm burdens were significantly higher, there were no differences in fecal egg counts compared with mMCP-1^{+/+} controls (11). As this initial observation could have been due to immunological differences as a consequence of genetic variability, the experiment was repeated in BALB/c F₁₀ mMCP-1^{-/-} and mMCP-1^{+/+} mice. Worm survival was monitored by fecal egg counts (Fig. 3 A). Mice in these same two groups were rechallenged by gavage with 200 adult worms 21 d after the first infection. This route of infection was chosen to avoid any pulmonary immune response normally triggered by subcutaneous inoculation with L₃. Fecal egg counts were monitored until 4 d after the second challenge, when egg counts had declined in the majority of animals (Fig. 3 A). No significant differences between the mMCP-1^{+/+} and mMCP-1^{-/-} fecal egg counts were observed during primary or secondary challenge infection, confirming the results of previous studies (11). Worm burdens in the two groups were assessed 3 d after secondary challenge but were also not significantly different (mMCP-1^{+/+}, mean = 23.1 [SE 11.6]; mMCP-1^{-/-}, mean = 8.0 [SE 3.5]).

Altered MMC Kinetics in Parasitized mMCP-1^{-/-} Mice. Earlier studies (11) suggested that infection with *N. brasiliensis* induced an augmented MMC response in mMCP-1^{-/-} mice compared with mMCP-1^{+/+} controls, although this could have reflected immunological differences between the two groups. Therefore, we investigated the mast cell

recruitment and distribution in congenic BALB/c mMCP-1^{-/-} and mMCP-1^{+/+} mice after *T. spiralis* infection.

The numbers of MMCs and submucosal mast cells (SMMCs) recorded in the jejunum 6, 14, and 18 d after primary infection of BALB/c F₇ mMCP-1^{-/-} and mMCP-1^{+/+} mice with *T. spiralis* (Fig. 1 A) are shown in Fig. 1, C and E, respectively. There was a trend toward greater numbers of MMCs in the mMCP-1^{-/-} mice on day 18 (Fig. 1 C) and significantly higher numbers of SMMCs on days 14 and 18 after infection (Fig. 1 E). There were significantly higher numbers of total mast cells ($P < 0.05$) in the jejunum of mMCP-1^{-/-} mice than the mMCP-1^{+/+} controls on day 18 after infection.

The numbers of MMCs and SMMCs in the jejunum were also compared in BALB/c F₁₀ mMCP-1^{-/-} and mMCP-1^{+/+} mice after primary infection with *T. spiralis* (Fig. 1 B) over a wider range of time points (Fig. 1, D and F). When compared with uninfected controls (day 0), the numbers of MMCs in infected animals were significantly increased ($P < 0.01-0.05$) at all times except day 1 (Fig. 1 D). Hyperplasia of MMCs was maximal during the period of nematode expulsion (days 14–16). MMCs in mMCP-1^{-/-} mice were more abundant than in the mMCP-1^{+/+} controls on days 14, 16, and 30, and this was significant on day 14 of infection ($P < 0.01$; Fig. 1 D). The percentages of intraepithelial MMCs decreased during the course of infection but were similar in mMCP-1^{+/+} and mMCP-1^{-/-}

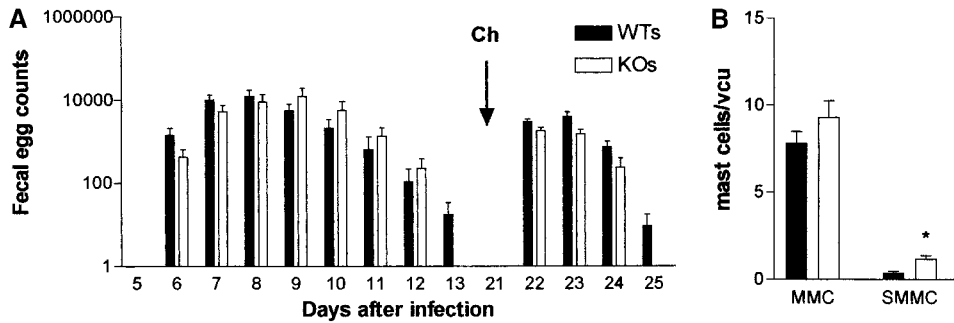


Figure 3. (A) Mean fecal egg counts ($\log_{10} [x + 1] + SE$) from mMCP-1^{+/+} (WTs) and mMCP-1^{-/-} (KOs) BALB/c F₁₀ mice after receiving a primary infection on day 0 with 500 *N. brasiliensis* larvae and challenge infection by gavage with 200 adult worms on day 21. (B) Mast cell counts (+SE) in the jejunum from mMCP-1^{+/+} (WTs) and mMCP-1^{-/-} (KOs) BALB/c F₁₀ mice 3 d after challenge infection with adult *N. brasiliensis*. See legend for Fig. 1, C and E.

mice (Table I). Recruitment of SMMCs was significant ($P < 0.01-0.05$) on days 14, 16, and 30 only when compared with uninfected controls (day 0; Fig. 1 F). Interestingly, there were significantly greater numbers of SMMCs in the jejunum of mMCP-1^{-/-} mice than in the mMCP-1^{+/+} controls on days 14 ($P < 0.01$), 16 ($P < 0.05$), and 30 ($P < 0.01$) after infection (Fig. 1 F). Overall, there were significantly more total mast cells in the mMCP-1^{-/-} mice than in the mMCP-1^{+/+} controls on days 14 ($P < 0.01$) and 30 ($P < 0.05$) after infection.

When mast cell hyperplasia was assessed in the jejunal mucosa and submucosa after challenge infection with *T. spiralis* (day 6 after infection), the numbers of MMCs in mMCP-1^{+/+} and mMCP-1^{-/-} mice were not significantly different (Fig. 2 B). However, there was generally a higher proportion of mast cells in the submucosa in jejunal sections from the mMCP-1^{-/-} mice (Fig. 2 D) than the mMCP-1^{+/+} controls (Fig. 2 C). When mast cell hyperplasia was assessed 4 d after challenge infection with *N. brasiliensis*,

the numbers of MMCs in mMCP-1^{+/+} and mMCP-1^{-/-} mice were again not significantly different, while the numbers of SMMCs were again significantly greater ($P < 0.05$) in the transgenics compared with wild-type controls (Fig. 3 B). The percentage of SMMCs in the jejunum of mMCP-1^{-/-} mice was significantly higher than mMCP-1^{+/+} controls in challenge infections with either *N. brasiliensis* or *T. spiralis* ($P < 0.01$; Table I). This and the previous data suggests an accumulation of mast cells in the submucosa during the phase of worm expulsion in both primary and challenge infections.

Expression and Systemic Release of mMCP-1 Correlates with Worm Expulsion. Concentrations of mMCP-1 in the jejunum and serum taken from both groups of mice during primary infection and during the expulsion phase of a challenge infection with *T. spiralis* were compared (Fig. 4, A and B). There was no detectable mMCP-1 in any of the samples from the mMCP-1^{-/-} mice (Fig. 4, A and B). During primary infection, concentrations of mMCP-1 in

Table I. Percentage Distribution of Mast Cells in the Jejunum of mMCP-1^{-/-} and mMCP-1^{+/+} Mice

			Percentage mast cells			
			Epithelium	Lamina propria	Submucosa	Muscularis
<i>T. spiralis</i> 1°	Day 6	WT	89 (3.5)	5 (2.5)	5 (3.1)	0.2 (0.2)
		KO	87 (4.4)	7 (2)	9 (6.3)	0.4 (0.4)
	Day 14	WT	80 (2.9)	10 (2.4)	9 (2.6)	0.5 (0.2)
		KO	75 (5)	15 (2.9)	9 (2.2)	1.5 (0.4)
	Day 30	WT	46 (5)	38 (5)	12 (3.5)	4 (1.5)
		KO	37 (1.8)	38 (2.5)	19 (1.1)	6 (0.9)
<i>T. spiralis</i> 2°	Day 6	WT	63 (4.2)	27 (2)	7.9 (1.2)	1 (0.2)
		KO	52 (2.3)	30 (1.2)	14.5** (1.6)	3 (0.8)*
<i>N. brasiliensis</i> 2°	Day 4	WT	74 (6.9)	21 (2.8)	3.7 (1.1)	0.6 (0.5)
		KO	70 (5.4)	15 (2.3)	10** (1.3)	4.7** (1)

The percentage of mast cells (+SE) counted in the epithelium, lamina propria, submucosa, and muscularis in the jejunum from mMCP-1^{+/+} (WT) and mMCP-1^{-/-} (KO) BALB/c F₁₀ mice after nematode infection. Data are shown for 6, 14, and 30 d after primary infection with *T. spiralis* muscle larvae (Fig. 1 B), 6 d after secondary challenge infection with *T. spiralis* (Fig. 2 A), and 3 d after secondary challenge infection with *N. brasiliensis* (Fig. 3 A). * $P < 0.05$ and ** $P < 0.01$, as referred to in text.

the jejunum or serum of mMCP-1^{+/+} mice on days 6–30 were all significantly higher ($P < 0.01$) than levels in uninfected controls. Fig. 4 A illustrates concentrations of mMCP-1 in jejunal homogenates, which peaked on day 15 and were 80–100-fold higher than in uninfected mMCP-1^{+/+} controls. However, concentrations of jejunal mMCP-1 6 d after secondary challenge were no greater than levels recorded 6 d after primary infection (Fig. 4 A), despite the increased MMC hyperplasia seen at this stage of challenge infection (Fig. 2 B). In contrast, levels recorded in the serum were significantly higher ($P < 0.01$) on day 6 after challenge than on day 6 after primary infection (Fig. 4 B). This data suggests that there is increased systemic release of mMCP-1 after challenge infection with *T. spiralis*.

Transcripts for *mMCP-1*, *mMCP-2*, and *mMCP-5* were compared by reverse transcription PCR in jejunal samples taken from uninfected mMCP-1^{-/-} and mMCP-1^{+/+} BALB/c F₁₀ mice on day 6 after challenge and on day 6 after primary infection (Fig. 4 C). No *mMCP-1* transcripts were detected in the jejunum from mMCP-1^{-/-} mice, but *mMCP-2* and *mMCP-5* appeared to be upregulated (Fig. 4 C), confirming earlier observations that transcription of these genes was apparently unaffected by *mMCP-1* deletion (11). However, levels of *mMCP-1* transcripts recorded 6 d after primary infection and 6 d after secondary challenge in the mMCP-1^{+/+} mice did not appear to be upregulated when compared with levels of transcription of GAPDH (Fig. 4 C).

Discussion

Here we show for the first time that the abundant and highly soluble MMC β -chymase, mMCP-1, is involved in

the immunological expulsion of nematode parasites from the intestine. Importantly, mMCP-1 appears to be required for efficient expulsion of *T. spiralis* primary (Fig. 1, A and B) and challenge infections (Fig. 2 A), but not for the expulsion of *N. brasiliensis* (Fig. 3 A). This is in accordance with the overwhelming evidence that expulsion of *T. spiralis* is highly dependent on MMCs and on the cytokines that regulate MMC hyperplasia and survival (13, 14, 18, 19). In contrast, expulsion of *N. brasiliensis* appears to be independent of mast cells in the mouse (20, 21).

Previous studies using bone marrow restoration of mast cell-deficient *c-kit* mutant mice (13) or treatment of mice with antibodies against *c-kit* (19) or stem cell factor (14) provided the strongest evidence for the involvement of mast cells in the rejection of nematodes. However, the interpretation of all such studies relies on an association between depletion/restoration of MMC populations and delayed/restored worm expulsion. Perhaps the most intriguing aspect of the current data is that delayed expulsion of *T. spiralis* occurred in mMCP-1^{-/-} mice, despite the observations showing MMC hyperplasia was equivalent or greater than that in the mMCP-1^{+/+} controls. Furthermore, this is the first report showing that the elimination of a 'downstream' effector molecule, uniquely derived from MMCs, affects the survival of a gut-dwelling nematode. It is not yet clear, however, whether the increased deposition of muscle larvae in mMCP-1^{-/-} mice was due to the persistence of the adult worms, increased worm fecundity, or a combination of these two elements.

The initial establishment and survival of *T. spiralis* larvae was comparable in both groups of mice, and only during the phase of worm loss were there any detectable differences in worm burdens between the mMCP-1^{-/-} and

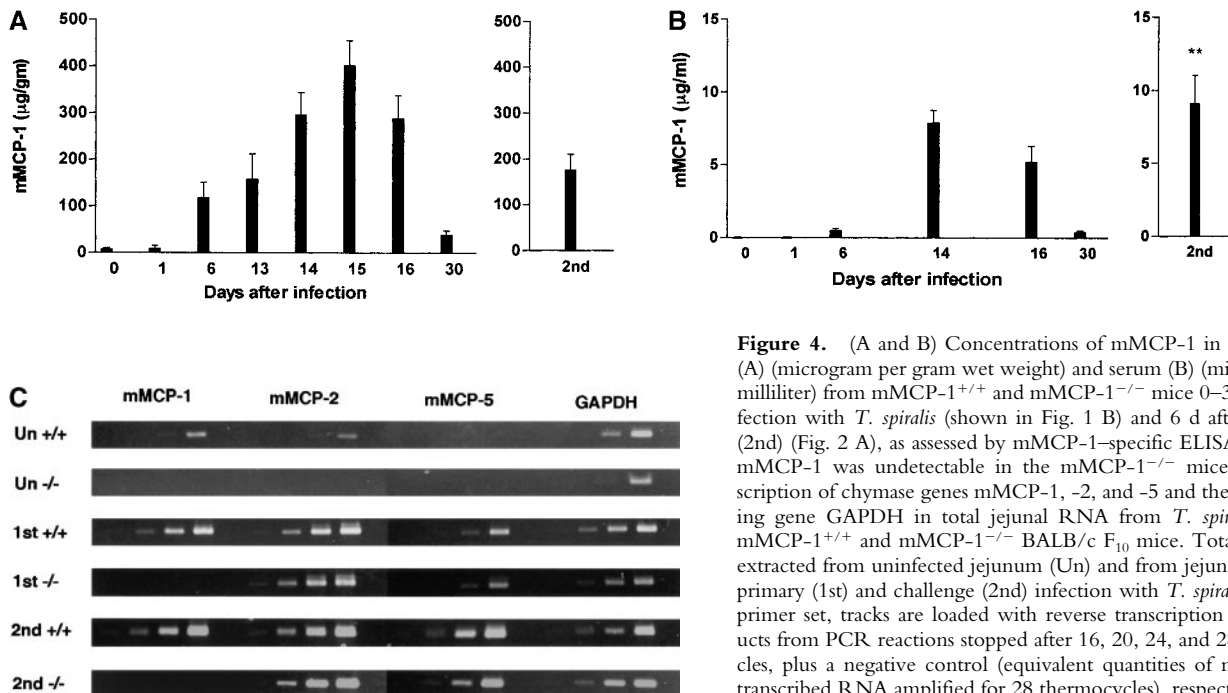


Figure 4. (A and B) Concentrations of mMCP-1 in the jejunum (A) (microgram per gram wet weight) and serum (B) (microgram per milliliter) from mMCP-1^{+/+} and mMCP-1^{-/-} mice 0–30 d after infection with *T. spiralis* (shown in Fig. 1 B) and 6 d after challenge (2nd) (Fig. 2 A), as assessed by mMCP-1-specific ELISA. Note that mMCP-1 was undetectable in the mMCP-1^{-/-} mice. (C) Transcription of chymase genes mMCP-1, -2, and -5 and the housekeeping gene GAPDH in total jejunal RNA from *T. spiralis* infected mMCP-1^{+/+} and mMCP-1^{-/-} BALB/c F₁₀ mice. Total RNA was extracted from uninfected jejunum (Un) and from jejunum 6 d after primary (1st) and challenge (2nd) infection with *T. spiralis*. For each primer set, tracks are loaded with reverse transcription PCR products from PCR reactions stopped after 16, 20, 24, and 28 thermocycles, plus a negative control (equivalent quantities of non-reverse-transcribed RNA amplified for 28 thermocycles), respectively.

mMCP-1^{+/+} controls. Extensive backcrossing onto a BALB/c background virtually eliminates the possibility that a susceptibility gene cosegregates with the mMCP-1^{-/-} genotype. Furthermore, our data on the transcription of mMCP-2 and -5 suggest that expression of these chymases is unaffected in mMCP-1^{-/-} mice (Fig. 4 C). The role of these other chymases in worm rejection has not been investigated. In view of their close relationship to each other on chromosome 14 (22), it is likely that mMCP-2, -4, and -5 are inherited as a complex from the 129 strain mouse embryonic stem cells used in the targeting of mMCP-1. As both mMCP-2 and -5 are apparently expressed normally in the BALB/c mMCP-1^{-/-} mice, it is unlikely that they influence the expulsion process.

Recent evidence suggests that during the resolution of MMC hyperplasia, MMCs in the jejunum migrate laterally and downwards into the submucosa and are sequestered in the spleen via the bloodstream (23, 24). The migration of MMCs from the villi to the crypts and submucosa is accompanied by an apparent change in phenotype from MMC-like to connective tissue mast cell-like (23). Therefore, the excessive abundance of MMC and the accumulation of SMMCs in the jejunum of mMCP-1^{-/-} mice during the later stages of nematode infection suggests a defect in the resolution of MMC hyperplasia in the absence of mMCP-1, rather than an increase in initial mast cell recruitment. Furthermore, as 90–95% of MMCs expressing mMCP-1 are intraepithelial and mMCP-1⁺ cells were absent from the submucosa (reference 9 and our unpublished observations), the altered mast cell hyperplasia is likely to be caused by an inability of mMCP-1^{-/-} cells to migrate or change phenotype or a downstream effect on other cells in the mucosa. While we have clearly demonstrated a role for a MMC β -chymase in nematode expulsion, the mechanisms by which it operates remain to be elucidated.

We thank Margaret McPhee and Liz Thornton for carrying out the mMCP-1 ELISAs, Jeremy Brown for his extensive help with digital imaging, and Anne Rosbottom and Tim Nuttal for the RNA extraction method. We also thank Cheryl Scudamore for helpful discussion and Eileen Duncan, Liz Moore, and Judith Pate for their technical support.

This work was supported by grants 050065 and 060312 from the Wellcome Trust.

Submitted: 13 October 2000

Accepted: 30 October 2000

References

1. Enerback, L. 1987. Mucosal mast cells in the rat and man. *Int. Arch. Allergy Appl. Immunol.* 82:249–253.
2. Befus, A.D., F.L. Pearce, J. Gaudie, P. Horsewood, and J. Bienstock. 1982. Mucosal mast cells 1. Isolation and functional characteristics of rat intestinal mast cells. *J. Immunol.* 128:2475–2480.
3. Miller, H.R.P., J.F. Huntley, G.F.J. Newlands, A. Mackellar, D.A. Lammas, and D. Wakelin. 1988. Granule proteases define mast cell heterogeneity in the serosa and gastrointestinal mucosa of the mouse. *Immunology.* 65:559–566.
4. Stevens, R.L., D.S. Friend, H.P. McNeil, V. Schiller, N. Ghildyal, and K.F. Austen. 1994. Strain-specific and tissue specific expression of mouse mast cell secretory granule proteases. *Proc. Natl. Acad. Sci. USA.* 91:128–132.
5. Woodbury, R.G., H.R.P. Miller, J.F. Huntley, G.F.J. Newlands, A.C. Palliser, and D. Wakelin. 1984. Mucosal mast cells are functionally active during spontaneous expulsion of intestinal nematode infections in the rat. *Nature.* 312:450–452.
6. Miller, H.R.P. 1996. Mucosal mast cells and the allergic response against nematode parasites. *Vet. Immunol. Immunopathol.* 54:331–336.
7. Scudamore C.L., A.M. Pennington, E.M. Thornton, L. McMillan, G.F.J. Newlands, and H.R.P. Miller. 1995. The release of the mucosal mast cell chymase, rat mast cell protease II, during anaphylaxis is associated with the rapid development of paracellular permeability to macromolecules in rat jejunum. *J. Exp. Med.* 182:1871–1881.
8. Scudamore, C.L., M.A. Jepson, B.H. Hirst, and H.R.P. Miller. 1998. The rat mucosal mast cell chymase, RMCP-II, alters epithelial cell monolayer permeability in association with altered distribution of the tight junction proteins ZO-1 and occludin. *Eur. J. Cell. Biol.* 75:321–330.
9. Scudamore, C.L., L. McMillan, E.M. Thornton, S.H. Wright, G.F.J. Newlands, and H.R.P. Miller. 1997. Mast cell heterogeneity in the gastrointestinal tract. Variable expression of mouse mast cell protease-1 (mMCP-1) in intraepithelial mucosal mast cells in nematode-infected and normal BALB/c mice. *Am. J. Pathol.* 150:1661–1672.
10. Huntley, J.F., C. Gooden, G.F.J. Newlands, A. Mackellar, D.A. Lammas, D. Wakelin, M. Tuohy, R.G. Woodbury, and H.R.P. Miller. 1990. Distribution of intestinal mast cell protease in blood and tissues of normal and *Trichinella*-infected mice. *Parasite Immunol.* 12:85–95.
11. Wastling, J.M., P. Knight, J. Ure, S. Wright, E.M. Thornton, C.L. Scudamore, J. Mason, A. Smith, and H.R.P. Miller. 1998. Histochemical and ultrastructural modification of mucosal mast cell granules in parasitized mice lacking the β -chymase, mouse mast cell protease-1. *Am. J. Pathol.* 153:491–504.
12. Urban, J.F., N. Noben-Trauth, D.D. Donaldson, K.B. Madden, S.C. Morris, M. Collins, and F.D. Finkelman. 1998. IL-13, IL-4Ra, and Stat6 are required for the expulsion of the gastrointestinal nematode parasite *Nippostrongylus brasiliensis*. *Immunity.* 8:255–264.
13. Ha, T.Y., N.D. Reed, and P.K. Crowle. 1983. Delayed expulsion of adult *Trichinella spiralis* by mast cell deficient W/W^v mice. *Infect. Immun.* 41:445–447.
14. Faulkner, H., N. Humphreys, J.C. Renaud, J. Van Snick, and R. Grecnis. 1997. Interleukin-9 is involved in host protective immunity to intestinal nematode infection. *Eur. J. Immunol.* 27:2536–2540.
15. Wakelin, D., and M.M. Wilson. 1977. Transfer of immunity to *Trichinella spiralis* in the mouse with mesenteric lymph node cells in donors and expression of immunity in recipients. *Parasitology.* 74:215.
16. Miller, H.R.P., and W.F.H. Jarrett. 1971. Immune reactions in mucous membranes. 1. Intestinal mast cell responses during helminth expulsion in the rat. *Immunology.* 20:227–288.
17. Wastling, J.M., C.L. Scudamore, E.M. Thornton, G.F.J. Newlands, and H.R.P. Miller. 1997. Constitutive expression of mouse mast cell protease-1 in normal BALB/c mice and its up-regulation during intestinal nematode infection. *Immu-*

- nology. 90:308–313.
18. Lawrence, C.E., J.C.M. Paterson, L.M. Higgins, T.T. MacDonald, M.W. Kennedy, and P. Garside. 1998. IL-4 regulated enteropathy in an intestinal nematode infection. *Eur. J. Immunol.* 28:2672–2684.
 19. Donaldson, L.E., E. Schmitt, J.F. Huntley, G.F.J. Newlands, and R.K. Grencis. 1996. A critical role for stem cell factor and *c-kit* in host protective immunity to an intestinal helminth. *Int. Immunol.* 8:559–567.
 20. Mitchell, L.A., R.B. Wescott, and L.E. Perryman. 1983. Kinetics of expulsion of the nematode, *Nippostrongylus brasiliensis*, in mast-cell deficient W/W^v mice. *Parasite Immunol.* 4:1–12.
 21. Nawa, Y., N. Ishikawa, K. Tsuchiya, Y. Horii, T. Abe, A. Khan, B. Shi, H. Itoh, H. Ide, and F. Uchiyama. 1994. Selective effector mechanisms for the expulsion of intestinal helminths. *Parasite Immunol.* 16:333–338.
 22. Gurish, M.F., J.H. Nadeau, K.R. Johnson, H.P. McNeil, K.M. Grattan, K.F. Austen, and R.L. Stevens. 1993. A closely linked complex of mouse mast cell-specific chymase genes on chromosome 14. *J. Biol. Chem.* 268:11372–11379.
 23. Friend, D.S., N. Ghildyal, K.F. Austen, M.F. Gurish, R. Matsumoto, and R.L. Stevens. 1996. Mast cells that reside at different locations in the jejunum of mice infected with *Trichinella spiralis* exhibit sequential changes in their granule ultrastructure and chymase phenotype. *J. Cell Biol.* 135:279–290.
 24. Friend, D.S., M.F. Gurish, K.F. Austen, J. Hunt, and R.L. Stevens. 2000. Senescent jejunal mast cells and eosinophils in the mouse translocate to the spleen and draining lymph node, respectively, during the recovery phase of helminth infection. *J. Immunol.* 165:344–352.